

Journal of Geophysical Research: Atmospheres

RESEARCH ARTICLE

10.1002/2017JD027021

Key Points:

- Urbanization impact on diurnal skin-surface temperature range is more complex than on diurnal surface air temperature range
- Diurnal skin-surface temperature range is inclined to be larger (smaller) in urban areas than in rural areas in summer (winter)
- Urban-rural difference in diurnal skin-surface temperature range is negatively related to the difference in vegetation abundance

Correspondence to:W. Zhan,
zhanwenfeng@nju.edu.cn**Citation:**

Huang, F., Zhan, W., Wang, Z., Wang, K., Chen, J. M., Liu, Y., ... Ju, W. (2017). Positive or negative? Urbanization-induced variations in diurnal skin-surface temperature range detected using satellite data. *Journal of Geophysical Research: Atmospheres*, 122, 13,229–13,244. <https://doi.org/10.1002/2017JD027021>

Received 23 APR 2017

Accepted 3 DEC 2017

Accepted article online 12 DEC 2017

Published online 27 DEC 2017

Positive or Negative? Urbanization-Induced Variations in Diurnal Skin-Surface Temperature Range Detected Using Satellite Data

Fan Huang¹ , Wenfeng Zhan^{1,2} , Zhihua Wang³ , Kaicun Wang⁴ , Jing M. Chen^{1,5}, Yongxue Liu⁶ , Jiameng Lai¹, and Weimin Ju^{1,2}

¹Jiangsu Provincial Key Laboratory of Geographic Information Science and Technology, International Institute for Earth System Science, Nanjing University, Nanjing, China, ²Jiangsu Center for Collaborative Innovation in Geographical Information Resource Development and Application, Nanjing, China, ³School of Sustainable Engineering and the Built Environment, Arizona State University, Tempe, AZ, USA, ⁴College of Global Change and Earth System Science, Joint Center for Global Change Studies, Beijing Normal University, Beijing, China, ⁵Department of Geography and Program in Planning, University of Toronto, Toronto, ON, Canada, ⁶Department of Geographic and Oceanographic Sciences, Nanjing University, Nanjing, China

Abstract Diurnal temperature range (DTR) is an important indicator for assessing the local climate change due to urbanization. Studies that focused on surface air temperature (SAT) have reported decreased DTR_{SAT} in urban areas. However, this urbanization-induced effect becomes more complex with regard to land skin-surface temperature (LST), which is highly localized and extremely sensitive to land surface properties. We thus investigated the urban-rural DTR_{LST} difference ($\Delta\text{DTR}_{\text{LST}}$) over 354 cities across China using satellite-retrieved LSTs within 2008–2013. Our major findings include the following: (1) urban areas experience increased (decreased) DTR_{LST} compared with rural areas on the annual average for the majority of cities located in southern (northern) China; (2) the $\Delta\text{DTR}_{\text{LST}}$ is mostly positive in warm months but negative in cold months. It generally becomes more positive from January to August and becomes more negative afterward; and (3) the $\Delta\text{DTR}_{\text{LST}}$ is positively related to the daytime surface urban heat island intensity; it is yet negatively correlated with the urban-rural difference in vegetation abundance. We consider these insights valuable for in-depth understanding urban thermal environment and will likely help improve urban planning.

1. Introduction

Simply defined as the difference between daily maximum and minimum temperatures, diurnal temperature range (DTR) is an important indicator for assessing climate change (Stocker, 2014). In the context of global warming, an increased DTR would probably occur when the daily maximum temperature increases more than minimum temperature, and vice versa. The DTR change may impose adverse impacts on the well-being of both humans and ecosystems. Reports have shown that a large DTR may risk human health by increasing mortality and morbidity, especially for the elderly and children (Cheng et al., 2014). Endotherms like birds also suffer from the impacts of a large DTR that can imperil their population viability (Briga & Verhulst, 2015). It is therefore of practical necessity to comprehensively understand the DTR variations to help with prediction and mitigation purposes.

Using long-term records of surface air temperature (SAT) and other associated meteorological parameters, the SAT-based DTR (DTR_{SAT}) variations caused by different factors such as the solar radiation (Wild, Ohmura, & Makowski, 2007), cloud and aerosol (Dai et al., 2006), water vapor (Stenchikov & Robock, 1995), and surface properties (Gallo, Easterling, & Peterson, 1996) have been studied at both regional and global scales (Braganza, Karoly, & Arblaster, 2004; Makowski, Wild, & Ohmura, 2008; Shen et al., 2014). Among these factors, the surface properties (e.g., albedo, surface roughness, moisture, and thermal inertia) act a notable role because they affect the land-atmosphere interaction (Feddema et al., 2005). Compared with the SAT, a parameter subject to near-surface atmospheric turbulence and mixing, the land surface temperature (LST) is more sensitive to surface properties. Therefore, the LST-based DTR (DTR_{LST}) variations are likely to differ from the DTR_{SAT} ones.

By converting natural land surfaces to urban (man-made) ones, urbanization greatly changes surface properties and results in an irreversible local climate change, which modifies the energy budgets and hydrologic

processes. Urban areas generally experience reduced incident solar radiation (Alpert & Kishcha, 2008), enhanced precipitation (Huff & Changnon, 1973), increased thermal inertia, surface roughness, anthropogenic heat and greenhouse gas emissions, and decreased evapotranspiration, among other local changes in surface characteristics and surface processes. These urbanization-induced conversions may, individually or collectively, cause the regional DTR_{SAT} and DTR_{LST} variations. A number of investigations have been conducted to evaluate the urbanization impacts on DTR_{SAT} (Gallo et al., 1996; Kalnay & Cai, 2003; Trusilova et al., 2008; Wang et al., 2012; Zhou et al., 2004; Zhou & Ren, 2011). Their findings include the following: (1) urbanization generally leads to a decrease in DTR_{SAT} compared with rural areas; (2) the decreased DTR_{SAT} directly results from the asymmetric responses of daily maximum and minimum temperatures to urbanization; and (3) very few studies reported increased DTR_{SAT} over urban areas (Zhou et al., 2004).

Characterized by extensive coverage as well as relatively high accuracy, satellite retrieved LST has been used to quantify the urbanization impacts on local DTR_{LST} . Using LST retrieved from the Geostationary Operational Environment Satellite over the U.S., Sun et al. (2006) observed that the DTR_{LST} is smaller in urban sites than in rural ones on average during an annual cycle. An increasing number of studies have been using LSTs retrieved from the Moderate Resolution Imaging Spectroradiometer (MODIS) onboard Terra/Aqua satellites for analysis. Mohan and Kandya (2015) found that the DTR_{LST} decreases due to urbanization in Delhi, India. A study by Lazzarini et al. (2015) similarly indicated that downtown areas show smaller DTR_{LST} than surrounding undeveloped areas for hot desert cities. However, Wang et al. (2007) reported that the DTR_{LST} difference between urban and rural areas in Beijing, China, could sometimes be positive across an annual cycle; that is, the DTR_{LST} might increase due to urbanization in some seasons.

While it is generally agreed that urbanization generally decreases DTR_{SAT} , the impact of urbanization on DTR_{LST} is still uncertain. LST differs from SAT on the associated mechanisms, though they are closely related (Good, 2016). The satellite-retrieved LST measures the radiance emitted by a surface, which shows high sensitivity over heterogeneous and nonisothermal surface types with different emissivities (Li et al., 2013), while in situ SAT appears more homogeneous due to near-surface atmospheric turbulence and mixing. Moreover, LST is usually several degrees greater than SAT by day under clear skies because the former is more sensitive to solar radiation, while they become relatively closer at the night. The urbanization-induced DTR_{LST} variations are therefore anticipated to be more complex than on DTR_{SAT} . This study investigates a large number of cities located in different geographical zones across China in order to improve our understanding of the impacts of urbanization on DTR_{LST} .

2. Materials and Methods

2.1. Study Area

We selected 354 cities across China in descending order of urban areas of at least 10 km^2 (Figure 1). These cities are distributed in six geographical zones (Fang et al., 2001), including the northwest (46 cities), north (37 cities), northeast (37 cities), southwest (40 cities), central south (88 cities), and east zones (106 cities). The altitude over mainland China generally decreases from west to east toward the sea. From south to north the climate changes through tropical, subtropical, warm temperate, mild temperate, and cold temperate zones. Generally, monsoon climates prevail in the southeast of China while continental climates dominate the northwest, resulting in humid, semihumid, semiarid, and arid climates from southeast to northwest.

2.2. Data

We used imageries and gridded data sets that include MODIS LST product MYD11A2, MODIS land cover product MCD12Q1, MODIS vegetation index product MYD13A2, and topographic elevation product GTOPO30. In order to obtain valid data without significant cloud influences, we collected the MODIS Collection 6 products for the 2008–2013 period. The MYD11A2 data were aggregated temporally from the daily LST product (i.e., MYD11A1) as the average of clear-sky LSTs during an 8 day period. The MODIS LST was retrieved from the brightness temperatures in bands 31 and 32 using a generalized split-window algorithm with the mean LST errors within $\pm 1 \text{ K}$ in most cases (Wan, 2014; Wan & Dozier, 1996). MYD11A2 provides 1 km LSTs at both daytime ($\sim 13:30 \text{ p.m. local solar time}$) and nighttime ($\sim 01:30 \text{ a.m.}$). The satellite-retrieved LSTs are only valid under clear-sky conditions. The MCD12Q1 data provide yearly 500 m land cover types, which contain five classification schemes derived through a supervised decision-tree classification method (Friedl et al., 2002). We used



Figure 1. Background land cover types extracted from MODIS product MCD12Q1 of 2013 and geographical zones of the selected 354 major cities across China.

the primary land cover scheme defined by the International Geosphere Biosphere Programme. The MYD13A2 data provide two vegetation indices in every 16 days at 1 km spatial resolution, that is, enhanced vegetation index (EVI) and normalized difference vegetation index (NDVI). We used EVI rather than NDVI because EVI minimizes background variations and removes residual atmosphere contamination (Clinton & Gong, 2013). The GTOPO30 is a global digital elevation model with a spatial resolution of 30 arc s (approximately 1 km).

The other data sets include in situ SAT data provided by China Meteorological Data Service Center and the associated weather records during 2012 for the six capital cities (Figure 2). The SAT data were recorded hourly at automatic meteorological observation sites spread across each city (Figure 2). They were marked separately as an urban or rural site (refer to section 2.3). The numbers of sites (total sites, urban sites, and rural sites) are (39, 15, 24) in Xian, (67, 32, 35) in Beijing, (8, 3, 5) in Harbin, (27, 11, 16) in Kunming, (63, 17, 46) in Wuhan, and (9, 5, 4) in Shanghai, respectively.

2.3. Methods

The urban and rural areas were defined using the land cover and elevation data. We resampled the gridded land cover data by nearest sampling and the elevation data by bilinear sampling to 1 km spatial resolution, the same as the LST data. The land cover and elevation data of each city were then extracted by the administrative boundary (Figure 1). Within the administrative border of a city, the pixels labeled as water, forests, snow and ice, and permanent wetlands were excluded due to their relatively small LST variations, and the pixels with an elevation ± 50 m off the median elevation of the urban pixels were also removed to reduce the LST differences due to elevation and shading (Imhoff et al., 2010). The median instead of mean elevation of the urban pixels within the city administrative borders was applied in order to eliminate some fragmentary

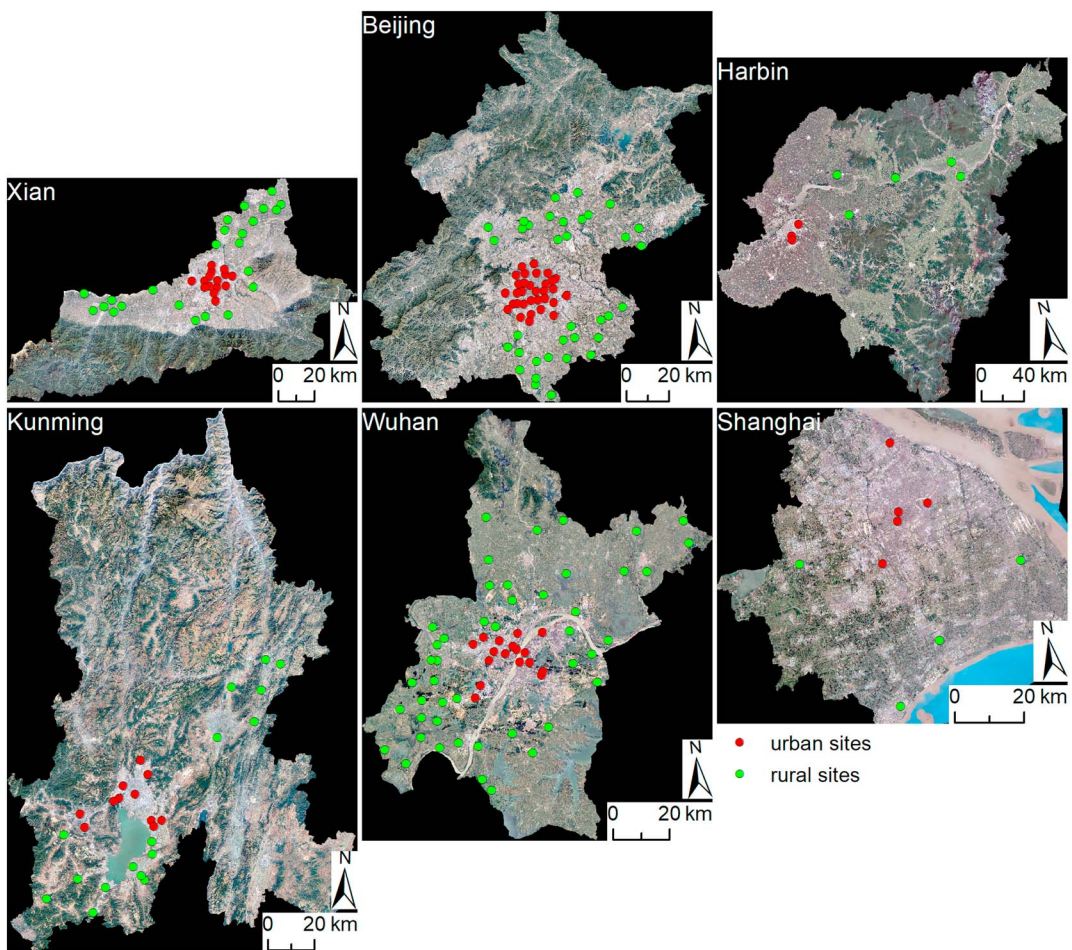


Figure 2. Distribution of automatic meteorological observation sites in Xian, Beijing, Harbin, Kunming, Wuhan, and Shanghai.

urban pixels that have an extreme high or low elevation. After the exclusion of pixels, the remaining urban pixels within the city boundaries were flagged as the urban areas, while the remaining nonurban pixels were flagged as the rural areas.

The urban-rural DTR difference ($\Delta\text{DTR}_{\text{LST}}$) was used to quantify the urbanization impacts on DTR_{LST} . For the representation of the clear-sky LST climatology during an annual cycle, we averaged the MODIS LST data of the same 8 day period over the 6 years, separately for daytime and nighttime. These averaged 8 day LST data were then aggregated by month for a general representation. The DTR_{LST} of a pixel was calculated as the difference between daytime and nighttime LSTs. The $\Delta\text{DTR}_{\text{LST}}$ of a city was calculated as the difference between the DTR_{LST} averaged over the urban pixels and that averaged over the rural pixels. By further averaging the month-to-month $\Delta\text{DTR}_{\text{LST}}$, we obtained the annual $\Delta\text{DTR}_{\text{LST}}$. To determine whether the $\Delta\text{DTR}_{\text{LST}}$ averaged over the cities in each geographical zone is significantly positive or negative at the 0.05 level, we used the one-sample t test (SPSS Statistics 23; Norušis, 2006) with 1,000 bootstrap samples, which also allowed us to estimate the bias-corrected 95% confidence interval containing the $\Delta\text{DTR}_{\text{LST}}$ mean. To interpret the urbanization impacts on DTR_{LST} , we calculated the urban-rural EVI difference (ΔEVI) by month for each city and also the urban-rural LST difference, that is, surface urban heat island intensity.

An urban or rural meteorological site was identified by where it is located, that is, whether the pixel a site located within is urban or rural. Most of the urban sites are located at downtown, while the rural sites are located at outer suburbs for the six cities (Figure 2). To distinguish the urbanization impacts on DTR_{LST} and DTR_{SAT} , we calculated the urban-rural DTR_{SAT} difference ($\Delta\text{DTR}_{\text{SAT}}$) under the clear-sky conditions and separately under the all-weather conditions. The clear days were selected according to the weather records. In

addition, we calculated by month the clear-sky/all-weather DTR_{SAT} at the site level and then calculated the clear-sky/all-weather ΔDTR_{SAT} at the city level. First, the SAT data on clear days during a month were averaged for each hour. Second, the clear-sky DTR_{SAT} of a site was calculated from the monthly clear-sky SAT data aggregated at each hour. Third, the clear-sky ΔDTR_{SAT} of a city was calculated as the difference between the averaged clear-sky DTR_{SAT} over the urban sites and that over the rural sites. The all-weather ΔDTR_{SAT} was calculated in a similar way using all-weather data instead of only clear-sky data. For comparison, the clear-sky ΔDTR_{LST} of each selected city was also calculated by month with the urban and rural pixels extracted from the site locations.

3. Results

3.1. Annual ΔDTR_{LST}

In general, the annual ΔDTR_{LST} is positive over half (56%) of these chosen cities, and there is a clear north-south contrast in the ΔDTR_{LST} spatial pattern (Figure 3). Urban areas experience larger DTR_{LST} than rural areas for only 29% of the cities located in the three northern zones, that is, the northwest (24% of the cities within this region), north (16%), and northeast (49%) zones, respectively. By comparison, this percentage rises to above 70% for the three southern zones, that is, the southwest (80%), central-south (57%), and east (76%) zones, respectively. The annual ΔDTR_{LST} averaged over all the cities in the northwest, north, and northeast zones is $-1.02 [-1.41, -0.64]$ K (in brackets is the 95% confidence interval), while it is $0.36 [0.24, 0.48]$ K averaged over all the cities in the southwest, central south, and east zones. The interannual variability may be assessed through the analysis of the annual ΔDTR_{LST} means, performed for each year within the study period (Figures A1 and A2 in Appendix A). The spatial variations of the annual ΔDTR_{LST} for each year are very similar. However, the year-to-year variability of the annual ΔDTR_{LST} is discernible, which may be associated to local factors (e.g., changes in land cover) or synoptic variability (e.g., year-to-year changes in cloud cover or incoming solar radiation).

Considering various rural background (i.e., the dominant rural land cover types) on which cities are situated, we further categorize the annual ΔDTR_{LST} by the rural background land cover types (Figure 3). Referring to Figure 1, the main land cover types of the rural background are grasslands (GL), barren or sparsely vegetated lands (BSV), and croplands (CL) for cities in the northwestern and northern zones; CL and cropland/natural vegetation mosaic lands (CNV) for cities in the northeastern and eastern zones; woody savannas (WS) and CL for cities in the southwestern zone; and CL, CNV, and WS for cities in the central south zone, respectively. We found that the annual ΔDTR_{LST} tends to be negative for the cities with GL or BSV background but positive for the cities with WS or CNV background. It shows greater variations for the cities with CL background. We also found that the topographic elevation modulates the local ΔDTR_{LST} to some extent as it may affect some other ecologic settings besides land cover. The annual DTR_{LST} shows a significantly positive correlation with the logarithm of elevation, while the annual ΔDTR_{LST} shows a weaker but still significantly negative correlation with the logarithm of elevation (refer to Figure B1 in Appendix B). Note that these correlations are influenced by the group of points with high elevations, which indicates that these relations may be nonlinear.

In the northwest zone, the annual ΔDTR_{LST} is negative for all the BSV cities, for most of the GL cities (16/21, i.e., 16 out of 21 cities), and for about half of the CL cities (7/13). The north zone also shows negative ΔDTR_{LST} for most of the GL (11/14) and CL (18/21) cities. For the cities with GL background, those (3/14) located at lower elevations than 500 m show positive ΔDTR_{LST} , while the cities with negative ΔDTR_{LST} (11/14) are located at higher altitudes. For the cities with CL background, those (12/21) located at elevations lower than 60 m show negative ΔDTR_{LST} . In the northeast zone, the ΔDTR_{LST} is positive for all the cities with CNV background, while it is negative for over half of the CL cities (18/32). In the southwest zone, all of the cities with WS or CNV background show positive ΔDTR_{LST} as well as most of the CL cities (22/29). The two GL cities show opposite ΔDTR_{LST} , a little positive for the one located at a lower elevation while negative for the other at a higher elevation. In the central south and east zones, the annual ΔDTR_{LST} is positive for most of the cities with WS, CL, or CNV background.

To further illustrate the underlying mechanisms governing the relationships between the annual ΔDTR_{LST} and rural background, we take a closer look at the two sample land cover types that generally lead to the opposite trends of ΔDTR_{LST} , namely, the BSV (i.e., barren or sparsely vegetated) and WS (i.e., woody savannas). Our results show that the annual DTR_{LST} is $13.9 [13.2, 14.6]$ K averaged over urban pixels, larger than 13.1

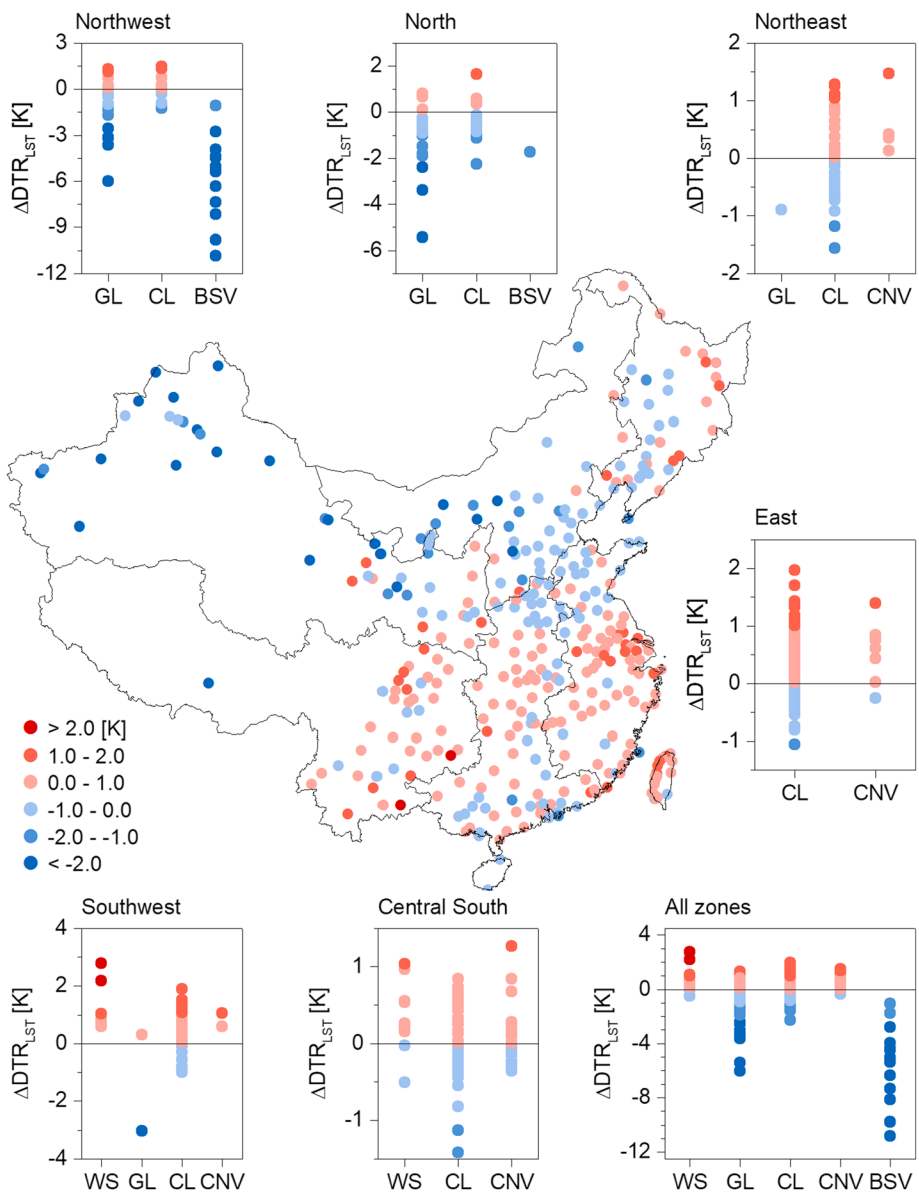


Figure 3. Spatial variations of the annual ΔDTR_{LST} and the classification of the annual ΔDTR_{LST} by rural background for the cities in each region. Each color-filled cycle indicates the annual ΔDTR_{LST} of a specific city. "WS," "GL," "CL," "CNV," and "BSV" represent the woody savannas, grasslands, croplands, cropland/natural vegetation mosaic lands, and barren or sparsely vegetated lands, respectively.

[12.5, 13.7] K averaged over rural pixels for the cities with WS background. By comparison, the annual DTR_{LST} averaged over urban pixels is smaller than that averaged over rural pixels (22.7 [21.5, 24.1] K versus 28.2 [27.1, 29.4] K) for the cities with BSV landscape. We examined the annual EVI, and the results illustrate that the urban pixels are less vegetated when compared with rural pixels (0.23 [0.22, 0.24] versus 0.31 [0.30, 0.32]) for the cities with WS landscape, whereas this situation is reversed (0.14 [0.11, 0.16] versus 0.07 [0.06, 0.08]) for the cities with BSV landscape. The surface roughness length of WS landscape is characteristically larger than BSV landscape but smaller than urban areas (Stull, 2015; Wiernga, 1993). More vegetation implies more evapotranspiration that tends to decrease DTR_{LST} . However, higher land surface roughness represents stronger land-atmosphere coupling and therefore enhanced turbulent fluxes (Oke, 2002; Stull, 2012), which tends to decrease DTR_{LST} . We therefore speculate that the vegetation effect (e.g., evapotranspiration) overcomes the surface roughness effect that leads to smaller DTR_{LST} over rural areas than urban areas for the cities with WS background. However, the vegetation effect is almost negligible for

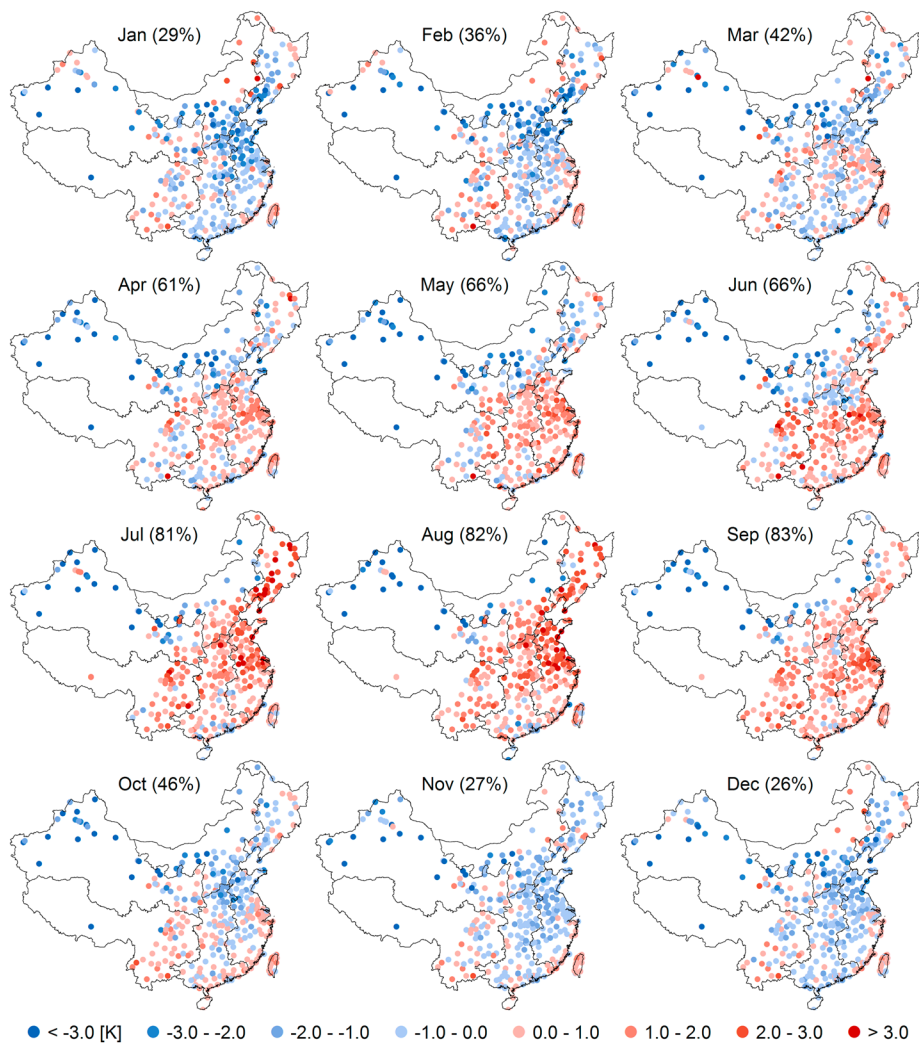


Figure 4. Spatiotemporal variations of the monthly ΔDTR_{LST} . The percentage at the top of each subfigure denotes the percentage of cities with positive ΔDTR_{LST} .

the cities with BSV background. The relatively low thermal inertia of the rural desert surfaces probably causes its larger DTR_{LST} than urban areas. A prominent example is that for cities located in arid environment, an urban oasis cooling effect is constantly observed in contrast to its barely vegetated surroundings, hence indicating a strongly negative ΔDTR_{LST} (Lazzarini et al., 2015). More quantitative discussions between the ΔDTR_{LST} and vegetation status will be further provided in section 4.1.

3.2. Monthly ΔDTR_{LST}

The monthly ΔDTR_{LST} also shows distinct spatiotemporal variations (Figure 4). Generally, the majority of cities show larger DTR_{LST} over urban areas compared with rural areas in the warm months from April to September, but the situation is reversed in the cold months. The percentage of cities with positive ΔDTR_{LST} increases from January to September and falls back in October to December. A typical contrast was also observed between the southeast and northwest regions during the warm months. The cities located in the northwest region show smaller DTR_{LST} over urban areas compared with rural areas, while larger DTR_{LST} appears over urban areas for the cities in the southeast region. In July and August, the monthly ΔDTR_{LST} is higher than 1.0 K for nearly half of the whole cities while higher than 2.0 K for around a quarter. By comparison, the ΔDTR_{LST} in January and February falls below -1.0 K for nearly 40% of the whole cities.

By averaging over all the cities, the monthly ΔDTR_{LST} is significantly positive in July (0.61 [0.32, 0.90] K), August (0.68 [0.40, 0.95] K), and September (0.43 [0.20, 0.65] K); it is close to 0.0 K (not significant at the

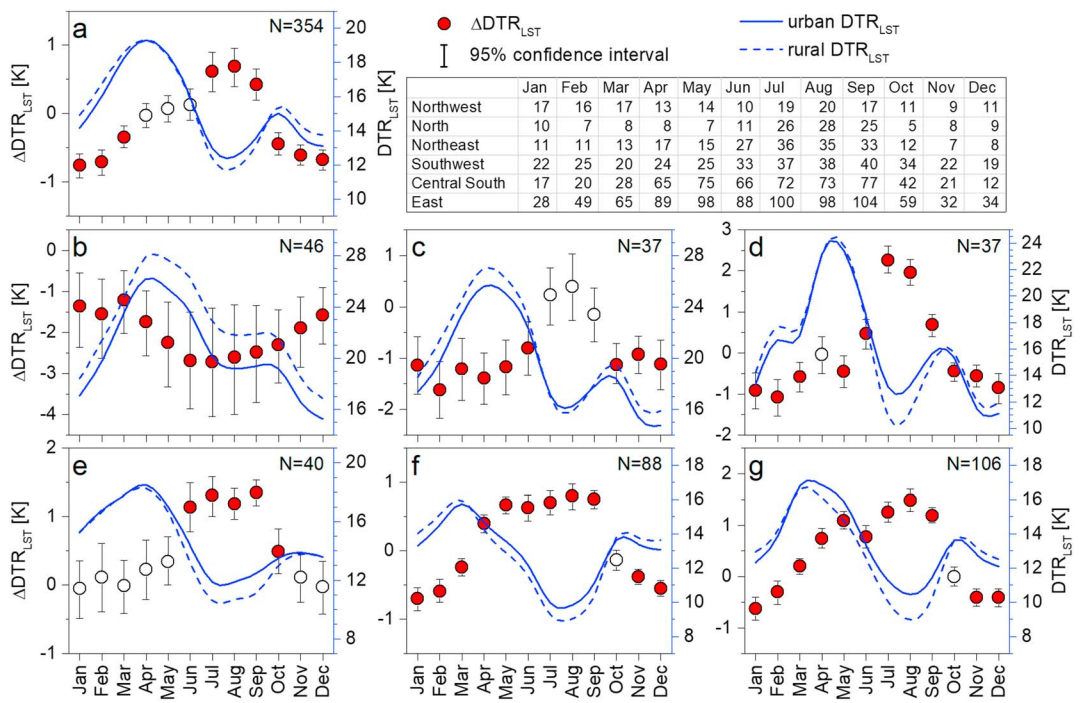


Figure 5. Monthly variations of the averaged ΔDTR_{LST} over the cities in (a) all zones, (b) northwest, (c) north, (d) northeast, (e) southwest, (f) central south, and (g) east zone, respectively. The averaged ΔDTR_{LST} marked by an unfilled circle is not significantly different from zero at the 0.05 level. N is the number of cities in each zone. The table shows the number of cities with positive ΔDTR_{LST} .

0.05 level) from April to June and becomes significantly negative from October to March (Figure 5a). These results confirm that urban areas tend to experience larger DTR_{LST} compared with rural surroundings in warm months while a reversed situation occurs in cold months. The monthly ΔDTR_{LST} generally increases from January to August and then decreases afterward. Such a trend remains for each geographical zone except the northwest zone. We also found that urbanization tends to increase DTR for a longer period in the three southern zones than the three northern zones.

In the northwest zone, nearly half of the cities (21/46) show smaller DTR_{LST} over urban areas compared with rural areas throughout the year (Figure 4). Five cities located in desert climate with BSV background, that is, Korla, Hotan, Turpan, Aksu, and Jiuquan, show negative ΔDTR_{LST} below -10.0 K in July and August, with one of them (i.e., Korla) reaching the minimum -12.8 K in February. However, four cities with CL background show positive ΔDTR_{LST} ranging within 1.1 to 2.4 K from June to September and two of them show larger DTR_{LST} over urban areas than rural areas throughout the year. The averaged ΔDTR_{LST} over this zone becomes more negative (at the 0.05 significance level) from January to July and then becomes less negative (Figure 5b). The negative ΔDTR_{LST} over the northwest zone is probably related to the desert arid climate. For these cities, the urban areas usually demonstrate an oasis cooling effect typified by a daytime (nighttime) surface urban cool (heat) island (Lazzarini et al., 2015), leading to a general negative ΔDTR_{LST} (more discussions are in section 4.1). In the north zone, the positive ΔDTR_{LST} accounts for less than 30% except in July (70%), August (76%), and September (68%) (Figure 4). The averaged ΔDTR over the cities in this zone is significantly negative before June and after October, while it is not significant from July to September (Figure 5c). For Beijing, the appearance of larger DTR_{LST} over urban areas than rural areas during summer is similar to those observed by Wang et al. (2007) and Huang et al. (2016). In the northeast zone, the majority of cities show positive ΔDTR_{LST} in July (97%), August (95%), and September (89%), but fewer than 30% of the cities show positive ΔDTR_{LST} from November to February (Figure 4). The averaged ΔDTR_{LST} over this zone is significantly positive from June to September, reaching 2.27 [1.95 , 2.60] K in July and 1.96 [1.66 , 2.28] K in August (Figure 5d).

In the southwest zone, nearly all of the cities show positive ΔDTR_{LST} from July to September (Figure 4). The averaged ΔDTR_{LST} over the cities in this zone is significantly positive from June (1.14 [0.78 , 1.49] K) to

September (1.35 [1.16, 1.53] K), but it is not significant (very close to 0.0 K) from December to March (Figure 5e), suggesting that, in the cold months, the urbanization impact on DTR is weak. In the central south and east zones, the majority of cities show positive $\Delta\text{DTR}_{\text{LST}}$ from April to September while negative $\Delta\text{DTR}_{\text{LST}}$ accounts for the majority from November to February (Figure 4). The averaged $\Delta\text{DTR}_{\text{LST}}$ generally increases from January to August and decreases subsequently, and it is not significantly different from zero in October (Figures 5f and 5g). Considering that the rural background land cover types play an important role in regulating the $\Delta\text{DTR}_{\text{LST}}$ variations, we additionally provided the monthly $\Delta\text{DTR}_{\text{LST}}$ variations grouped by the main background land cover instead of the geographical zone. The associated results are presented by Figure C1 in Appendix C.

4. Discussion

4.1. Analysis of $\Delta\text{DTR}_{\text{LST}}$ Variations

The urban-rural difference in local thermal environment, which can be well represented by surface urban heat island (SUHI), is probably associated to the local $\Delta\text{DTR}_{\text{LST}}$ variations. We thus provide the statistical relationships between $\Delta\text{DTR}_{\text{LST}}$ and daytime/nighttime SUHI intensity (SUHII) by month over all the cities (Figure 6). Our results show that the correlation between $\Delta\text{DTR}_{\text{LST}}$ and SUHII is generally stronger in the daytime than nighttime except in December. The Pearson's correlation (r) between $\Delta\text{DTR}_{\text{LST}}$ and daytime SUHII reaches 0.9 from May to September, while it is slightly smaller in January (0.75) and December (0.63). This suggests that there exists a significant and positive relationship between the $\Delta\text{DTR}_{\text{LST}}$ and daytime SUHII. In other words, a weak or negative daytime SUHII probably provokes a negative $\Delta\text{DTR}_{\text{LST}}$, especially for those cities shown in Figure 4, where the negative $\Delta\text{DTR}_{\text{LST}}$ always appears around winter or over desert arid climate zones. Comparatively, the $\Delta\text{DTR}_{\text{LST}}$ is generally negatively related to nighttime SUHII, although the relationships are much weaker than for daytime SUHII. The Pearson's r ranges between -0.55 and -0.80 from October to March. Their relationships remain significant in April, May, June, and September despite weaker correlations, but not significant in July and August at the 0.05 level as indicated by p values.

The urban thermal environment can be to some extent attributed to the change of land surface biophysical properties (Stone et al., 2013). Such changes can be partly characterized by the urban-rural difference in vegetation abundance. We therefore provide the correlations between $\Delta\text{DTR}_{\text{LST}}$ and ΔEVI by month over all the cities (Figure 7). The results clarify that there exist statistically significant negative linear correlations between $\Delta\text{DTR}_{\text{LST}}$ and ΔEVI across an annual cycle except in January. The negative relations are understandable as daytime SUHII has been shown to be negatively related to vegetation indices (Peng et al., 2011). From April to October, the negative relationships are significant at the 0.05 level, with Pearson's $r < -0.5$ and p value < 0.05 . Within this period, the EVI is smaller in urban areas than rural surroundings for most cities, leading to lower rural LSTs during daytime caused by more evapotranspiration, and this subsequently results in a decreased $\Delta\text{DTR}_{\text{LST}}$ over rural areas when compared with urban areas. By comparison, a few cities experience significantly positive ΔEVIs (i.e., urban areas show larger EVI than rural areas) from May to September, which are mostly located in the northwest zone with the rural surroundings covered by desert steppes. The positive ΔEVI that generally results in urban oasis cooling effect and the relatively low thermal inertia of rural background probably contribute to the negative $\Delta\text{DTR}_{\text{LST}}$ for these cities. From December to February, the ΔEVI varies only in a small range around zero for most cities, which can be explained by vegetation phenology (e.g., defoliation) during the cold period. The statistical relationship between $\Delta\text{DTR}_{\text{LST}}$ and ΔEVI is weak during these months, even not significant at the 0.05 level for January. The ΔEVI can therefore only explain a small portion of the $\Delta\text{DTR}_{\text{LST}}$ variations, and this may be because the minimum LSTs (usually during the night) over urban are more impacted by other factors in addition to the EVI (e.g., such as the urban canyon effect and anthropogenic heat) (Zhou et al., 2011).

As mentioned in section 1, all the factors that contribute to the urban thermal environment will likely affect the $\Delta\text{DTR}_{\text{LST}}$ variations. These factors generally include the differences in vegetation abundance between urban and rural locations, decreased thermal inertia of building materials, solar radiation trapped in street canyons, increased anthropogenic heat emissions, and intensified clouds and aerosols, etc. Note that the impacts of clouds and aerosols are not included in this study because only clear-sky LSTs were retrieved by satellite thermal remote sensing. Our results show that the EVI difference between urban and rural areas statistically explains about 50% of the $\Delta\text{DTR}_{\text{LST}}$ variations from May to September, which indicates that the

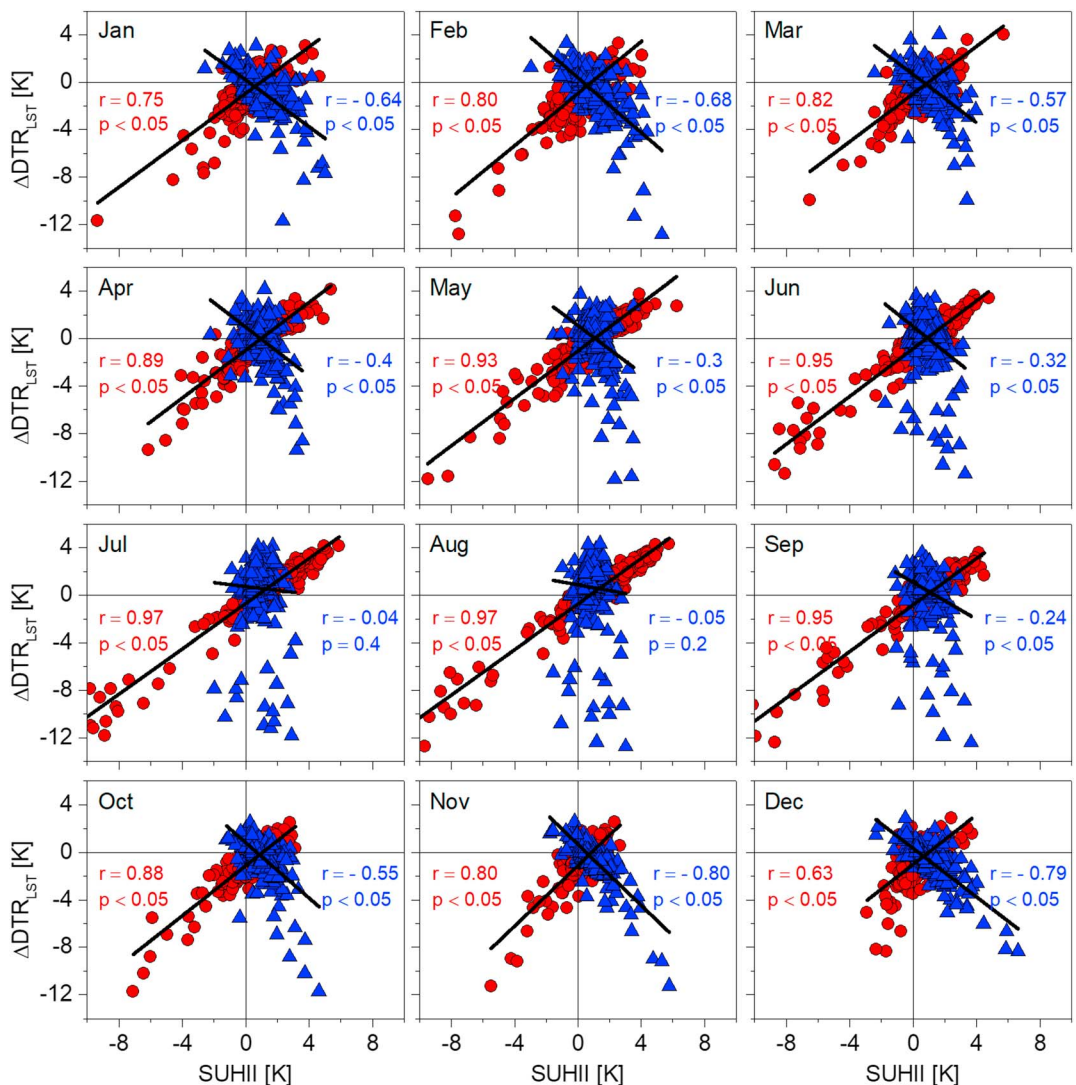


Figure 6. Correlations between the monthly ΔDTR_{LST} and daytime (red) and nighttime (blue) SUHII over all the cities. The p value smaller than 0.05 indicates that the positive/negative correlation is statistically significant at the 0.05 level.

surface biophysical properties play a major role in regulating the ΔDTR_{LST} variations during the warm months. Although the factors other than the vegetation abundance may be difficult to quantify for each city, such as the urban canyon effect and anthropogenic heat, these factors are probably more important in cold months. The relationships between these factors and the ΔDTR_{LST} variations deserve more investigations for future studies.

4.2. ΔDTR_{LST} Versus ΔDTR_{SAT}

Despite the consensus among previous studies that urbanization generally decreases DTR_{SAT} (Kalnay & Cai, 2003; Wang et al., 2012; Zhou et al., 2004), our results show that the urbanization-induced ΔDTR_{LST} has noteworthy seasonal variations and varies with cities located in different geographic zones. Urbanization may either increase or decrease DTR_{LST} ; for example, the annual ΔDTR_{LST} is positive (negative) for most cities in the east (northwest) zone (Figure 3) and the majority of cities experience positive (negative) ΔDTR_{LST} in warm (cold) months (Figure 4). In this study, we also provide a quantitative comparison between the ΔDTR_{SAT} and ΔDTR_{LST} variations for the six capital cities (Figure 8). These results again confirm that the ΔDTR_{LST} generally appears negative in cold months but positive in warm months. For Beijing and Shanghai, the seasonal variations of ΔDTR_{LST} are similar to the results reported by Wang et al. (2007) and Huang et al. (2016), in spite of the slightly different ΔDTR_{LST} ranges due to the selection of years and rural background. By comparison, in Xian,

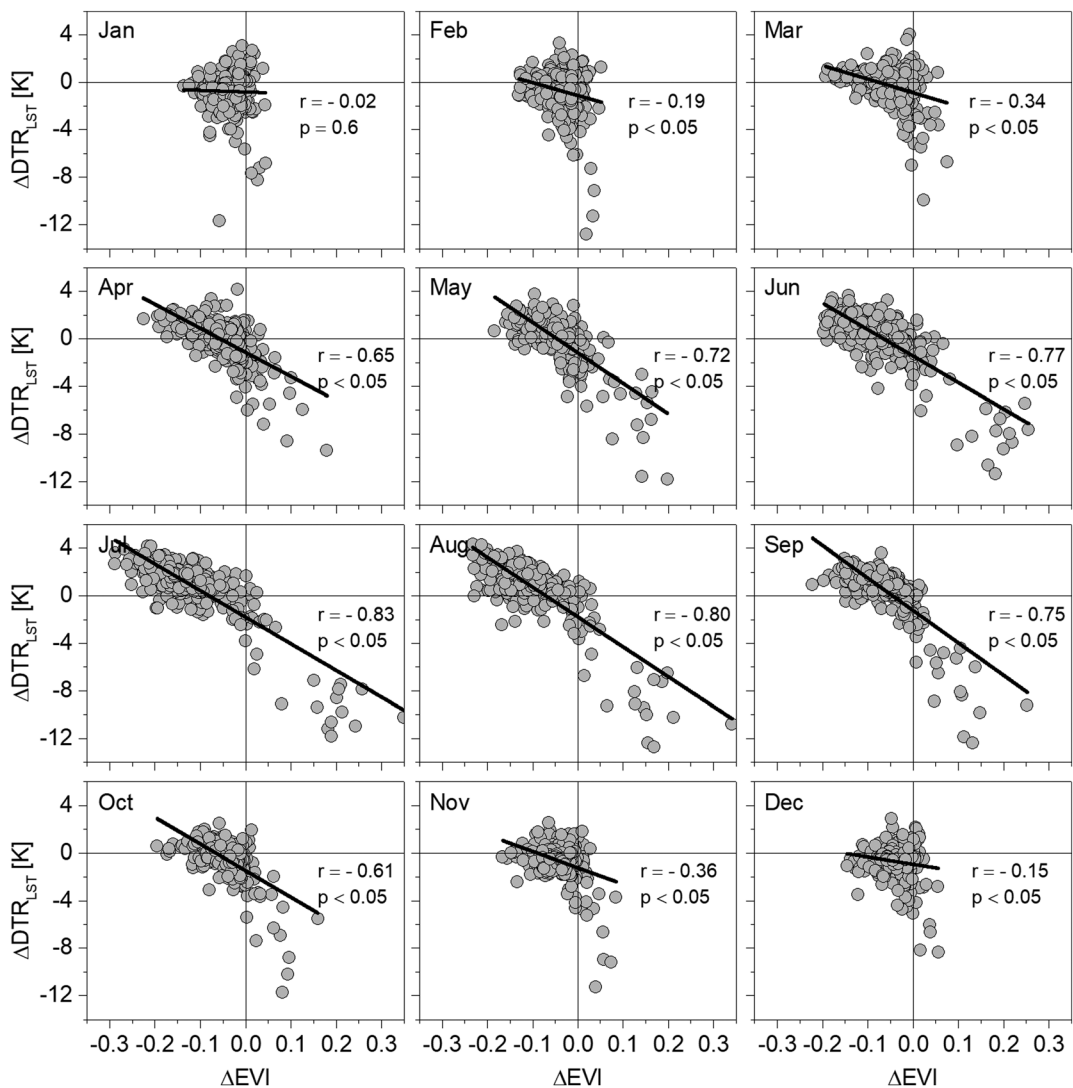


Figure 7. Correlations between the monthly ΔDTR_{LST} and ΔEVI over all the cities. The p value smaller than 0.05 indicates that the positive/negative correlation is statistically significant at the 0.05 level.

Beijing, Harbin, Kunming, and Wuhan, the mean monthly ΔDTR_{SAT} remains negative during the entire annual cycle (i.e., urbanization decreases DTR_{SAT}). In Shanghai, the ΔDTR_{SAT} is positive from March to August. We speculate that this is likely because the rural stations are affected by the nearby sea surface temperature that has a much smaller DTR (e.g., through coastal wind effects). Our results also show that the ΔDTR_{SAT} is generally more negative in all-weather than clear-sky conditions, interestingly indicating that the urban-rural DTR_{SAT} difference becomes smaller on cloudy/rainy than on clear-sky days.

The difference between ΔDTR_{LST} and ΔDTR_{SAT} can be traced back to the linked yet different phenomena between the surface urban heat island (LST-based, termed SUHI) and canopy layer urban heat island (SAT-based, termed CUHI) (Wang et al., 2017). The CUHI is commonly more pronounced during the nighttime than daytime, while daytime SUHI has a high probability to be stronger than at nighttime (Oke, 1982; Voogt & Oke, 2003). Considering that (1) the diurnal range of SUHI (CUHI) intensity approximates to the ΔDTR_{LST} (ΔDTR_{SAT}) (Wang et al., 2007) and (2) the CUHI and SUHI intensities are approximately comparable at nighttime in many cases (Anniballe, Bonafoni, & Pichierri, 2014), the more complex regime of ΔDTR_{LST} than ΔDTR_{SAT} , therefore, can be partly traced back to the different magnitudes between daytime (e.g., at solar noon) SUHI and CUHI. From typical urban (e.g., impervious) to surrounding rural (e.g., vegetated) surfaces, the urban-rural LST difference at around solar noon is expected higher than the associated SAT difference. This is because

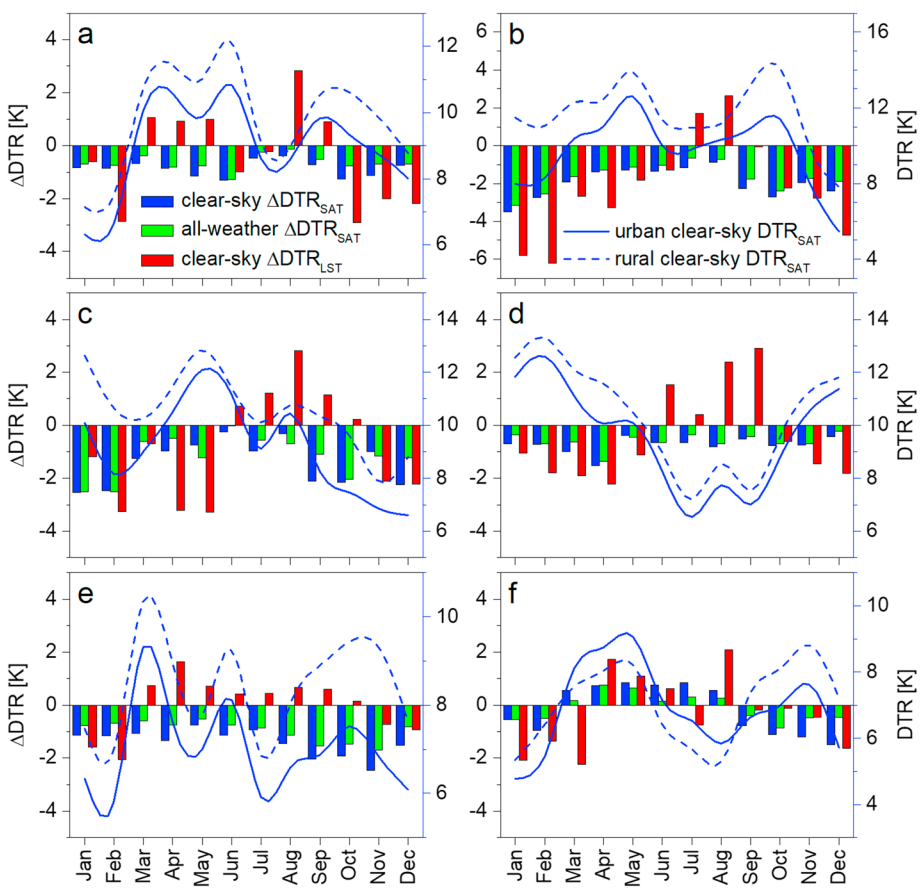


Figure 8. Monthly variations of the clear-sky ΔDTR_{SAT} , all-weather ΔDTR_{SAT} , and clear-sky ΔDTR_{LST} for the six capital cities. (a) Xi'an, (b) Beijing, (c) Harbin, (d) Kunming, (e) Wuhan, and (f) Shanghai.

daytime LST is highly localized and extremely sensitive to the surface properties, while SAT is more subject to atmospheric turbulence and mixing (Good, 2016). In short, it is mainly the notable daytime urban-rural LST difference that contributes to ΔDTR_{LST} probably becoming positive, when compared with the acknowledged negative urbanization-induced ΔDTR_{SAT} .

4.3. Uncertainties

The MODIS LST errors (within ± 1 K in most cases) would cause uncertainties in our results. First, the satellite-retrieved LST is usually affected by conditional bias, which suggests that the differences between daytime and nighttime LST errors do not necessarily cancel each other in calculating DTR_{LST} . Second, although the LST errors due to atmospheric effects might be greatly canceled out through subtraction, the LST errors due to emissivity over different land cover types (e.g., urban and nonurban) may not be consistent, and therefore, they may either cancel each other or instead be amplified in calculating ΔDTR_{LST} . Finally, we have to emphasize that the spatiotemporal patterns of ΔDTR_{LST} obtained in this study are restricted to clear-sky conditions, because satellite-retrieved LSTs are only valid on such days. If days with heavy clouds/aerosols/precipitation are included, the ΔDTR_{LST} variations may be even more complex than those reported herein. It is anticipated that the all-weather ΔDTR_{LST} may have a lower probability to be positive, because the differences between LST and SAT are smaller on cloudy than on clear days (Good, 2016).

5. Conclusions

The urbanization impacts on diurnal temperature range (DTR) are not yet well understood with regard to land skin-surface temperature (LST). This study is motivated to investigate the spatiotemporal dynamics of the urban-rural DTR_{LST} difference (ΔDTR_{LST}) over 354 major cities across China using satellite-derived LSTs.

New insights were gained. First, urban areas tend to experience larger DTR_{LST} compared with rural areas in warm months (e.g., July and August), while a reversed situation occurs in cold months (e.g., January and December), except for the cities located in the desert arid climate that generally show smaller DTR_{LST} over urban areas than rural areas throughout the year. Second, the ΔDTR_{LST} generally becomes more positive from January to around August and then becomes more negative afterward. Third, the ΔDTR_{LST} variations are positively related to the daytime surface urban heat island intensity and such variations can be partly explained by the urban-rural EVI difference (ΔEVI). This study provides a comprehensive analysis of the local DTR_{LST} change over a variety of cities with different geographical backgrounds. We consider that our study can help city planners to predict the urbanization-induced DTR_{LST} variations, therefore facilitating the development of measures to mitigate its adverse effects.

Appendix A: Interannual ΔDTR_{LST} Variations From 2008 to 2013 and the Significance of the Interannual Variability

Figure A1 shows the interannual ΔDTR_{LST} variations from 2008 to 2013. Figure A2 shows the significance status on whether the statistically mean value of the annual ΔDTR_{LST} over the 6 years is significantly different from zero at the 0.05 level.

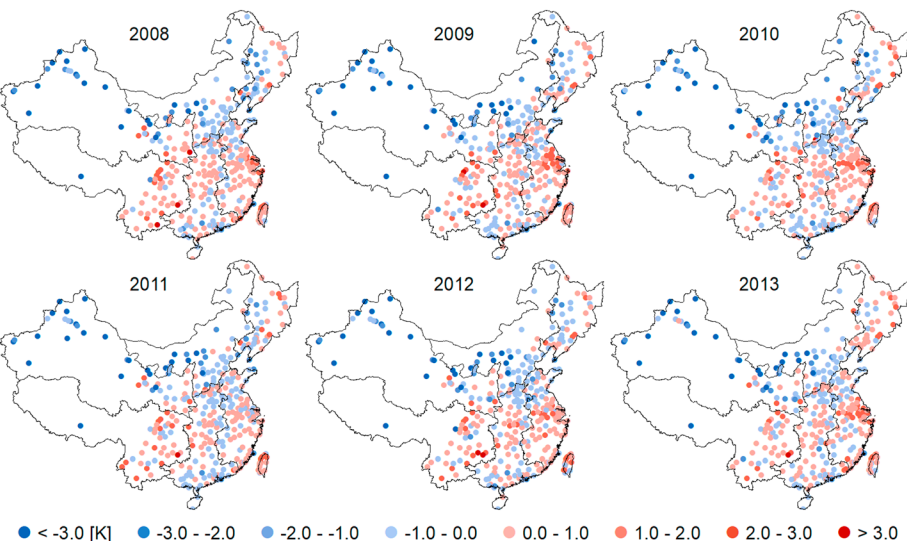


Figure A1. The interannual ΔDTR_{LST} variations from 2008 to 2013.

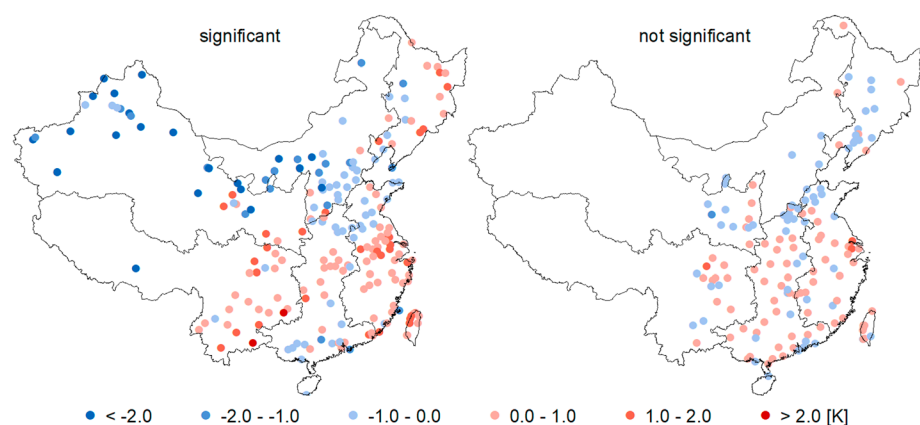


Figure A2. The significance status on whether the statistically mean value of the annual ΔDTR_{LST} over the 6 years is significantly different from zero at the 0.05 level.

Appendix B: Relations Between the Annual DTR_{LST} / ΔDTR_{LST} and Elevation

Figure B1 shows that the annual DTR_{LST} has a significantly positive correlation with the logarithm of elevation, while the annual ΔDTR_{LST} shows a weaker but significantly negative correlation with the logarithm of elevation.

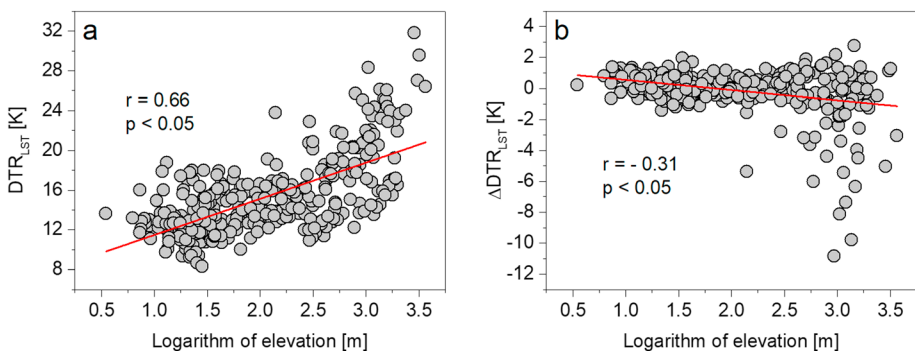


Figure B1. Relationships between the logarithm of elevation and the annual (a) DTR_{LST} and (b) ΔDTR_{LST} over all the cities.

Appendix C: Monthly Variations of the ΔDTR_{LST} Averaged Over the Cities Grouped by the Main Background Land Cover

Figure C1 provides the results similar to Figure 5 but grouped by the background land cover instead of geographical zone. Within the annual cycle, the urban DTR_{LST} tends to be larger than rural DTR_{LST} for the cities with the rural background covered mainly by woody savannas, while this situation is reversed for the cities with the main background land cover of grasslands or barren or sparsely vegetated lands.

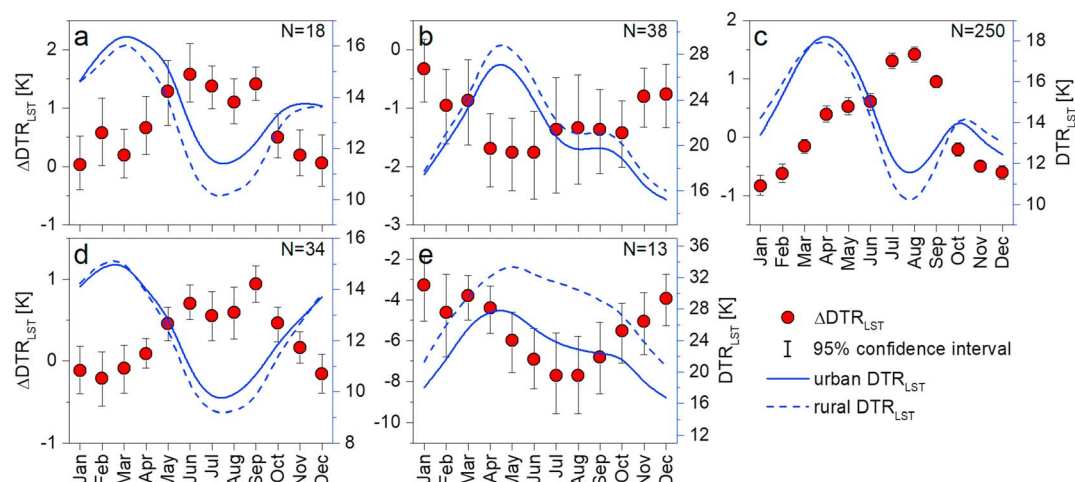


Figure C1. Monthly variations of the averaged ΔDTR_{LST} over the cities grouped by the main background land cover of (a) woody savannas, (b) grasslands, (c) croplands, (d) cropland/natural vegetation mosaic lands, and (e) barren or sparsely vegetated lands, respectively. N is the number of cities.

References

- Alpert, P., & Kishcha, P. (2008). Quantification of the effect of urbanization on solar dimming. *Geophysical Research Letters*, 35, L08801. <https://doi.org/10.1029/2007GL033012>
- Anibalbe, R., Bonafoni, S., & Pichierri, M. (2014). Spatial and temporal trends of the surface and air heat island over Milan using MODIS data. *Remote Sensing of Environment*, 150, 163–171. <https://doi.org/10.1016/j.rse.2014.05.005>
- Braganza, K., Karoly, D. J., & Arblaster, J. (2004). Diurnal temperature range as an index of global climate change during the twentieth century. *Geophysical Research Letters*, 31, L13217. <https://doi.org/10.1029/2004GL019998>

Acknowledgments

The authors would like to thank all the institutions that provide the data used in this study. The MODIS data were downloaded from NASA's Earth Observing System and Data and Information System (<https://earthdata.nasa.gov/>). The GTOPO30 elevation data were download from U.S. Geological Survey (USGS) EarthExplorer (<https://earthexplorer.usgs.gov/>). The hourly surface air temperature data were provided by China Meteorological Data Service Center. The ArcGIS 10.3 and SPSS Statistics 23 were used for analysis. This work is jointly supported by the National Natural Science Foundation of China under grant 41671420 and the Key Research and Development Programs for Global Change and Adaptation under grants 2016YFA0600201 and 2017YFA0603604. We are also grateful for the financial support provided by the DengFeng Program-B of Nanjing University.

- Briga, M., & Verhulst, S. (2015). Large diurnal temperature range increases bird sensitivity to climate change. *Scientific Reports*, 5(1), 16,600. <https://doi.org/10.1038/srep16600>
- Cheng, J., Xu, Z., Zhu, R., Wang, X., Jin, L., Song, J., & Su, H. (2014). Impact of diurnal temperature range on human health: A systematic review. *International Journal of Biometeorology*, 58(9), 2011–2024. <https://doi.org/10.1007/s00484-014-0797-5>
- Clinton, N., & Gong, P. (2013). MODIS detected surface urban heat islands and sinks: Global locations and controls. *Remote Sensing of Environment*, 134, 294–304. <https://doi.org/10.1016/j.rse.2013.03.008>
- Dai, A., Karl, T. R., Sun, B., & Trenberth, K. E. (2006). Recent trends in cloudiness over the United States: A tale of monitoring inadequacies. *Bulletin of the American Meteorological Society*, 87, 597–606. <https://doi.org/10.1175/BAMS-87-5-597>
- Fang, J., Chen, A., Peng, C., Zhao, S., & Ci, L. (2001). Changes in forest biomass carbon storage in China between 1949 and 1998. *Science*, 292(5525), 2320–2322. <https://doi.org/10.1126/science.1058629>
- Feddema, J. J., Oleson, K. W., Bonan, G. B., Mearns, L. O., Buja, L. E., Meehl, G. A., & Washington, W. M. (2005). The importance of land-cover change in simulating future climates. *Science*, 310, 1674–1678. <https://doi.org/10.1126/science.1118160>
- Friedl, M. A., McIver, D. K., Hodges, J. C. F., Zhang, X. Y., Muchoney, D., Strahler, A. H., ... Schaaf, C. (2002). Global land cover mapping from MODIS: Algorithms and early results. *Remote Sensing of Environment*, 83(1–2), 287–302. [https://doi.org/10.1016/S0034-4257\(02\)00078-0](https://doi.org/10.1016/S0034-4257(02)00078-0)
- Gallo, K. P., Easterling, D. R., & Peterson, T. C. (1996). The influence of land use/land cover on climatological values of the diurnal temperature range. *Journal of Climate*, 9(11), 2941–2944. [https://doi.org/10.1175/1520-0442\(1996\)009%3C2941:TIOLUC%3E2.0.CO;2](https://doi.org/10.1175/1520-0442(1996)009%3C2941:TIOLUC%3E2.0.CO;2)
- Good, E. J. (2016). An in situ-based analysis of the relationship between land surface "skin" and screen-level air temperatures. *Journal of Geophysical Research: Atmospheres*, 121, 8801–8819. <https://doi.org/10.1002/2016JD025318>
- Huang, F., Zhan, W., Voogt, J. A., Hu, L., Wang, Z., Quan, J., ... Guo, Z. (2016). Temporal upscaling of surface urban heat island by incorporating an annual temperature cycle model: A tale of two cities. *Remote Sensing of Environment*, 186, 1–12. <https://doi.org/10.1016/j.rse.2016.08.009>
- Huff, F. A., & Changnon, S. A. (1973). Precipitation modification by major urban areas. *Bulletin of the American Meteorological Society*, 54(12), 1220–1232. [https://doi.org/10.1175/1520-0477\(1973\)054%3C1220:pmbmua%3E2.0.co;2](https://doi.org/10.1175/1520-0477(1973)054%3C1220:pmbmua%3E2.0.co;2)
- Imhoff, M. L., Zhang, P., Wolfe, R. E., & Bounoua, L. (2010). Remote sensing of the urban heat island effect across biomes in the continental USA. *Remote Sensing of Environment*, 114, 504–513. <https://doi.org/10.1016/j.rse.2009.10.008>
- Kalnay, E., & Cai, M. (2003). Impact of urbanization and land-use change on climate. *Nature*, 423(6939), 528–531. <https://doi.org/10.1038/nature01675>
- Lazzarini, M., Molini, A., Marpu, P. R., Ouarda, T. B., & Ghedira, H. (2015). Urban climate modifications in hot desert cities: The role of land cover, local climate, and seasonality. *Geophysical Research Letters*, 42, 9980–9989. <https://doi.org/10.1002/2015GL066534>
- Li, Z.-L., Tang, B.-H., Wu, H., Ren, H., Yan, G., Wan, Z., ... Sobrino, J. A. (2013). Satellite-derived land surface temperature: Current status and perspectives. *Remote Sensing of Environment*, 131, 14–37. <https://doi.org/10.1016/j.rse.2012.12.008>
- Makowski, K., Wild, M., & Ohmura, A. (2008). Diurnal temperature range over Europe between 1950 and 2005. *Atmospheric Chemistry and Physics*, 8, 6483–6498. <https://doi.org/10.5194/acp-8-6483-2008>
- Mohan, M., & Kandya, A. (2015). Impact of urbanization and land-use/land-cover change on diurnal temperature range: A case study of tropical urban airshed of India using remote sensing data. *Science of the Total Environment*, 506–507, 453–465. <https://doi.org/10.1016/j.scitotenv.2014.11.006>
- Norušis, M. J. (2006). *SPSS 14.0 guide to data analysis*. Upper Saddle River, NJ: Prentice Hall.
- Oke, T. R. (1982). The energetic basis of the urban heat island. *Quarterly Journal of the Royal Meteorological Society*, 108(455), 1–24. <https://doi.org/10.1002/qj.49710845502>
- Oke, T. R. (2002). *Boundary layer climates* (2nd ed.). Oxford: Routledge.
- Peng, S., Piao, S., Ciais, P., Friedlingstein, P., Ottle, C., Bréon, F. O.-M., ... Myneni, R. B. (2011). Surface urban heat island across 419 global big cities. *Environmental Science & Technology*, 46, 696–703. <https://doi.org/10.1021/es2030438>
- Shen, X., Liu, B., Li, G., Wu, Z., Jin, Y., Yu, P., & Zhou, D. (2014). Spatiotemporal change of diurnal temperature range and its relationship with sunshine duration and precipitation in China. *Journal of Geophysical Research: Atmospheres*, 119, 13,163–13,179. <https://doi.org/10.1002/2014JD022326>
- Stenchikov, G. L., & Robock, A. (1995). Diurnal asymmetry of climatic response to increased CO₂ and aerosols: Forcings and feedbacks. *Journal of Geophysical Research: Atmospheres*, 100(D12), 26,211–26,227. <https://doi.org/10.1029/95JD02166>
- Stocker, T. F. (2014). *Climate change 2013: The physical science basis: Working Group I contribution to the fifth assessment report of the Intergovernmental Panel on Climate Change*. Cambridge: Cambridge University Press.
- Stone, B., Vargo, J., Liu, P., Hu, Y., & Russell, A. (2013). Climate change adaptation through urban heat management in Atlanta, Georgia. *Environmental Science & Technology*, 47(14), 7780–7786. <https://doi.org/10.1021/es304352e>
- Stull, R. (2012). *An introduction to boundary layer meteorology*. Dordrecht, Netherlands: Kluwer Academic.
- Stull, R. (2015). *Meteorology for scientists and engineers* (3rd ed.). Pacific Grove: Brooks Cole.
- Sun, D., Kafatos, M., Pinker, R. T., & Easterling, D. R. (2006). Seasonal variations in diurnal temperature range from satellites and surface observations. *IEEE Transactions on Geoscience and Remote Sensing*, 44, 2779–2785. <https://doi.org/10.1109/TGRS.2006.871895>
- Trusilova, K., Jung, M., Churkina, G., Karstens, U., Heimann, M., & Claussen, M. (2008). Urbanization impacts on the climate in Europe: Numerical experiments by the PSU-NCAR mesoscale model (MM5). *Journal of Applied Meteorology and Climatology*, 47, 1442–1455. <https://doi.org/10.1175/2007JAMC1624.1>
- Voogt, J. A., & Oke, T. R. (2003). Thermal remote sensing of urban climates. *Remote Sensing of Environment*, 86(3), 370–384. [https://doi.org/10.1016/S0034-4257\(03\)00079-8](https://doi.org/10.1016/S0034-4257(03)00079-8)
- Wan, Z. (2014). New refinements and validation of the collection-6 MODIS land-surface temperature/emissivity product. *Remote Sensing of Environment*, 140, 36–45. <https://doi.org/10.1016/j.rse.2013.08.027>
- Wan, Z., & Dozier, J. (1996). A generalized split-window algorithm for retrieving land-surface temperature from space. *IEEE Transactions on Geoscience and Remote Sensing*, 34(4), 892–905. <https://doi.org/10.1109/36.508406>
- Wang, K., Jiang, S., Wang, J., Zhou, C., Wang, X., & Lee, X. (2017). Comparing the diurnal and seasonal variabilities of atmospheric and surface urban heat islands based on the Beijing urban meteorological network. *Journal of Geophysical Research: Atmospheres*, 122, 2131–2154. <https://doi.org/10.1002/2016JD025304>
- Wang, K., Wang, J., Wang, P., Sparrow, M., Yang, J., & Chen, H. (2007). Influences of urbanization on surface characteristics as derived from the Moderate-Resolution Imaging Spectroradiometer: A case study for the Beijing metropolitan area. *Journal of Geophysical Research*, 112, D22S06. <https://doi.org/10.1029/2006JD007997>
- Wang, K., Ye, H., Chen, F., Xiong, Y., & Wang, C. (2012). Urbanization effect on the diurnal temperature range: Different roles under solar dimming and brightening. *Journal of Climate*, 25, 1022–1027. <https://doi.org/10.1175/JCLI-D-10-05030.1>

- Wiernga, J. (1993). Representative roughness parameters for homogeneous terrain. *Boundary-Layer Meteorology*, 63(4), 323–363. <https://doi.org/10.1007/bf00705357>
- Wild, M., Ohmura, A., & Makowski, K. (2007). Impact of global dimming and brightening on global warming. *Geophysical Research Letters*, 34, L04702. <https://doi.org/10.1029/2006GL028031>
- Zhou, J., Chen, Y., Wang, J., & Zhan, W. (2011). Maximum nighttime urban heat island (UHI) intensity simulation by integrating remotely sensed data and meteorological observations. *IEEE Journal of Selected Topics in Applied Earth Observations and Remote Sensing*, 4, 138–146. <https://doi.org/10.1109/JSTARS.2010.2070871>
- Zhou, L., Dickinson, R. E., Tian, Y., Fang, J., Li, Q., Kaufmann, R. K., ... Myneni, R. B. (2004). Evidence for a significant urbanization effect on climate in China. *Proceedings of the National Academy of Sciences of the United States of America*, 101, 9540–9544. <https://doi.org/10.1073/pnas.0400357101>
- Zhou, Y., & Ren, G. (2011). Change in extreme temperature event frequency over mainland China, 1961–2008. *Climate Research*, 50, 125–139. <https://doi.org/10.3354/cr01053>